




## ARTICLE

# Live reporting for hypoxia: Hypoxia sensor–modified mesenchymal stem cells as in vitro reporters

Carola Schmitz<sup>1</sup>  | Iliyana Pepelanova<sup>1</sup> | Dror Seliktar<sup>2</sup>  | Ekaterina Potekhina<sup>3</sup> | Vsevolod V. Belousov<sup>4,5</sup> | Thomas Scheper<sup>1</sup> | Antonina Lavrentieva<sup>1</sup> 

<sup>1</sup>Institute of Technical Chemistry, Gottfried Wilhelm Leibniz University Hannover, Hannover, Germany

<sup>2</sup>Faculty of Biomedical Engineering, Technion, Haifa, Israel

<sup>3</sup>Shemyakin-Ovchinnikov Institute of Bioorganic Chemistry, Moscow, Russia

<sup>4</sup>Center for Precision Genome Editing and Genetic Technologies for Biomedicine, Pirogov Russian National Research Medical University, Moscow, Russia

<sup>5</sup>Federal Center of Brain Research and Neurotechnologies, Federal Medical Biological Agency, Moscow, Russia

## Correspondence

Antonina Lavrentieva, Institute of Technical Chemistry, Gottfried Wilhelm Leibniz University Hannover, Callinstr. 5, 30167 Hannover, Germany.  
 Email: Lavrentieva@iftc.uni-hannover.de

## Funding information

Deutsche Forschungsgemeinschaft, Grant/Award Number: DFG Project 398007461 488 “3D Dual-Gradient Systems for Functional Cell Screening”; Ministry of Science and Higher Education of the Russian Federation, Grant/Award Number: 075-15-2019-1789; Niedersächsisches Ministerium für Wissenschaft und Kultur, Grant/Award Number: SMART BIOTECS

## Abstract

Natural oxygen gradients occur in tissues of biological organisms and also in the context of three-dimensional (3D) in vitro cultivation. Oxygen diffusion limitation and metabolic oxygen consumption by embedded cells produce areas of hypoxia in the tissue/matrix. However, reliable systems to detect oxygen gradients and cellular response to hypoxia in 3D cell culture systems are still missing. In this study, we developed a system for visualization of oxygen gradients in 3D using human adipose tissue–derived mesenchymal stem cells (hAD-MSCs) modified to stably express a fluorescent genetically engineered hypoxia sensor HRE-dUnaG. Modified cells retained their stem cell characteristics in terms of proliferation and differentiation capacity. The hypoxia-reporter cells were evaluated by fluorescence microscopy and flow cytometry under variable oxygen levels (2.5%, 5%, and 7.5% O<sub>2</sub>). We demonstrated that reporter hAD-MSCs output is sensitive to different oxygen levels and displays fast decay kinetics after reoxygenation. Additionally, the reporter cells were encapsulated in bulk hydrogels with a variable cell number, to investigate the sensor response in model 3D cell culture applications. The use of hypoxia-reporting cells based on MSCs represents a valuable tool for approaching the genuine in vivo cellular microenvironment and will allow a better understanding of the regenerative potential of AD-MSCs.

## KEYWORDS

3D cell culture, AD-MSCs, hydrogels, hypoxia sensor, reporter cells

## 1 | INTRODUCTION

Mesenchymal stem cells (MSCs) are widely used in medicine and clinical research due to their promising bioregenerative potential. At the moment, there are over 900 listed clinical trials recruiting MSCs of different origins for the treatment of various diseases and conditions (<http://www.clinicaltrials.gov>). Moreover, about 6,000 research and review articles about MSCs are published every year. The most promising strategy for using MSCs in bioregenerative

medicine is their application as cell suspensions for stromal/paracrine effects (trophic rescue function and immunomodulation) as well as employment of MSCs in tissue engineering and related applications (Han et al., 2019). Despite the existence of many encouraging results, the efficiency and reproducibility of treatment, as well as the survival of MSCs after implantation, are still very debated topics (Cheng, Chen, Li, & Young, 2013; Choi, Yong, & Wan Safwani, 2017; Fábíán, 2019; Haque, Rahman, Abu Kasim, & Alabsi, 2013; Lukomska et al., 2019).

This is an open access article under the terms of the Creative Commons Attribution License, which permits use, distribution and reproduction in any medium, provided the original work is properly cited.

© 2020 The Authors. *Biotechnology and Bioengineering* published by Wiley Periodicals LLC

Earlier, it was demonstrated that the cultivation of MSCs under hypoxic conditions increases cell proliferation (Lavrentieva, Majore, Kasper, & Hass, 2010), retention of stemness (Yamamoto et al., 2013), immunomodulatory activity, as well as MSC efficiency and survival after implantation (X. Hu et al., 2008). Moreover, cells cultivated under hypoxia demonstrate a completely different expression profile as compared to MSCs cultivated in ambient oxygen concentration (Lönne, Lavrentieva, Walter, & Kasper, 2013). While research agree about the significance of limited oxygen supply in stem cell expansion and preconditioning, the term “hypoxia” itself is only loosely and sometimes controversially defined. Inconsistencies in the terminology regarding what “normoxia” and what “hypoxia” are, came historically from the fact that the term “normoxia” was transferred to cell culture from physiology with no regard of the lower normal in vivo tissue O<sub>2</sub> concentrations (Bahsoun, Coopman, Forsyth, & Akam, 2018; Ivanovic, 2009). An oxygen concentration that is similar to the in vivo microenvironment is often referred to as physiological hypoxia or “physioxia” for a specific cell type, therefore “hypoxia” is defined as the condition under which this cell type is deprived of typical in vivo oxygen levels (Bahsoun et al., 2018; Koh & Powis, 2012). This definition sounds reasonable, but considering the many different MSC sources (e.g., umbilical cord, adipose tissue, bone marrow, and so forth), the range of physiological oxygen levels vary greatly (Pattappa, Johnstone, Zellner, Docheva, & Angele, 2019) and complicate a universal application of the term “hypoxia.” We do agree with Wenger, Kurtcuoglu, Scholz, Marti, and Hoogewijs (2015), who suggested a simple and adequate definition of hypoxia as “every decrease in pO<sub>2</sub> that causes a biological effect, for example, a (transient) increase in hypoxia inducible factor 1 $\alpha$  (HIF $\alpha$ ) protein stability.”

An explanation of the positive influence of hypoxic culture conditions on MSCs might be that these conditions are physiologically similar to the existing in vivo oxygen concentrations. Indeed, only few cell types in the body are exposed to atmospheric oxygen concentration—keratinocytes and melanocytes in the epidermis, pneumocytes and macrophages in lung alveoli, and cells of the corneal epithelium. Depending on the source, MSCs grow and function under low oxygen concentrations (Ejtehadifar et al., 2015). The major regulator of cell response to hypoxia is the HIF-1 $\alpha$ , a transcriptional factor, which consists of an  $\alpha$  and a  $\beta$  subunit (Jiang, Rue, Wang, Roe, & Semenza, 1996). HIF-1 $\alpha$  is constantly produced and degraded in the cell via ubiquitination. If oxygen concentration in the cell decreases, HIF-1 $\alpha$  stabilizes, associates with the HIF-1 $\beta$  subunit to form a heterodimer, and binds to hypoxia-responsive elements (HREs) of DNA, regulating the expression of over 300 genes in the process (Gaber, Dziurla, Tripmacher, Burmester, & Buttgerit, 2005; Schödel et al., 2011). In oxygen-rich environments, HIF-1 $\alpha$  gets degraded through hydroxylation and ubiquitination, which involves factor-inhibiting hypoxia-inducible factors and HIF prolyl hydroxylases (PHD) as well as the Von Hippel–Lindau tumor suppressor protein pVHL (Maxwell et al., 1999).

There are two standard strategies to modulate hypoxia in vitro: one is chemical simulation with mimicking agents (e.g., CoCl<sub>2</sub> or PHD inhibitors) and the second one—oxygen displacement in the

incubator or incubation chamber with nitrogen or argon. The chemical method can be used for some experimental setups where HIFs must be stabilized to investigate subjects related to the main regulatory hypoxia pathways (Pagé, Robitaille, Pouyssegur, & Richard, 2002). This method, however, is not suitable for expansion or in vitro cultivation of stem cells for bioregenerative applications. Oxygen displacement is a more physiological way to create hypoxic conditions, since the required “chemical hypoxia” reagents for HIF stabilization do not appear in vivo and might alter cellular behavior or be cytotoxic on the long term. Oxygen displacement involves broader spectrum of mechanisms, which can lead to indirect HIF stabilization or act even beyond it with all resulting implications on cellular behavior and metabolism (Bahsoun et al., 2018; Chakraborty et al., 2019; Pugh & Ratcliffe, 2017).

The implementation of hypoxia is an important way to approach true physiological conditions for MSCs. However, environmental factors other than oxygen can also be important. For example, the use of three-dimensional (3D) cell culture, where cells are embedded in a matrix and can form cell–cell, as well as cell–material contacts in 3D, could help maintain stem cell properties. Hydrogels, long chains of hydrophilic polymers, are frequently used for 3D cell cultivation. There is a large variety of natural, semi-synthetic, and synthetic hydrogels available for 3D cell culture, which have been designed over the last years (Pepelanova, Kruppa, Scheper, & Lavrentieva, 2018; Ruedinger, Lavrentieva, Blume, Pepelanova, & Scheper, 2015). They differ in their physiological properties, such as stiffness, pore sizes, and the ability to provide a cell-promoting environment (Malda et al., 2013). To create solid constructs and encapsulate cells, hydrogels undergo a sol–gel transition through a variety of crosslinking methods, for example, temperature shift, photopolymerization, or enzymatic crosslinking (W. Hu, Wang, Xiao, Zhang, & Wang, 2019). Regardless of the type of material or crosslinking method, literature lists many examples of MSC cultivation in hydrogels. However, the hydrogel construct sizes, as well as the cell-seeding number vary greatly in published studies, and the effects of these factors on the resulting oxygen concentrations experienced by the cells in situ remain unknown (Figueiredo et al., 2018). Bearing in mind that over 300 MSC genes experience oxygen-dependent regulation, it is essential that tools are urgently developed to elucidate how HIF-1 $\alpha$  stabilization functions in different contexts of 3D cell culture cultivation.

For this reason, we envision that the visualization of in situ hypoxia in 3D cell culture will become a valuable readout, in addition to standard live–dead staining and cell viability assays. One way to achieve this is through the use of reporter cell systems. The applications of hypoxia-reporter cells include the creation of hypoxic conditions in 3D cell cultures without oxygen displacement in incubators, but by a direct tuning of cell-seeding number and hydrogel composition. Using such constructs with in situ hypoxia allows a much better control of the cellular microenvironment and will be helpful in improving the reproducibility of tissue engineering protocols, as well as in vitro cell models in, for example, drug screening, tumor models, or cell behavior studies. An additional application of a

hypoxia sensor cell line would be the precise location of hypoxic regions in larger 3D structures, such as bioprinted or tissue-engineered cell constructs.

Recently, a novel type of hypoxia-sensor was reported, which contains HREs and the UnaG protein (Erapanedi, Belousov, Schäfers, & Kiefer, 2016). The maturation of the green fluorescent UnaG protein does not depend on oxygen and thus possesses an advantage over the commonly used green fluorescent protein (GFP; Kumagai et al., 2013). With the help of this sensor, it was possible to visualize a stabilization of HIF-1 $\alpha$  in two-dimensional (2D) cultures of human embryonic kidney (HEK) and Chinese hamster ovary (CHO) cells and to even follow the behavior of these cells after implantation in vivo (Erapanedi et al., 2016).

In this study, we report for the first time the creation of a lentivirally transduced hypoxia-reporter MSCs derived from human adipose tissue (hAD), based on this novel hypoxia-reporter system. In the present study, we describe the creation of the reporter cells, as well as the characterization of sensor properties under different conditions of 2D cell culture. Also, we have used hydrogels as a 3D cell culture platform to demonstrate how different cell-seeding densities and hydrogel types relate to the sensor hypoxic response. The use of hypoxia-reporting cells based on MSCs will allow researchers to come one step closer to the cultivation of MSCs in conditions resembling the genuine in vivo microenvironment.

## 2 | METHODS

### 2.1 | Isolation and cultivation of hAD-MSCs

hAD-MSCs were isolated from the adipose tissue of a 27-year old female donor after abdominoplasty using a protocol developed by Zhu et al. (2008). Briefly, fat tissue was cut in pieces with sterile scissors, approximately 20 ml (17–20 g) was transferred into a 50-ml tube and minced in the tube with sterile scissors to an almost homogeneous pulp. Ten milliliter of collagenase-CLS I solution (2 mg/ml in Hank's balanced salt solution; Merck, Darmstadt, Germany) was then added to each 20 ml of homogenate and incubated overnight at 4°C. Afterwards, homogenates were washed with Hank's balanced salt solution followed by centrifugation (5 min;  $\times 200g$ ). After centrifugation, the middle layer was discarded and resuspended pellet with fatty supernatant was washed twice with Hank's balanced salt solution containing 10% human serum (CC-pro, Oberdorla, Germany). The resulting pellet was resuspended in 50-ml cell culture medium and 25 ml suspension was transferred to each of two T175 cell culture flasks. Once cell colonies grew subconfluent and the cells covered the bottom surface of the flask, the cells were further subcultivated and cryopreserved. The patient had given her informed consent, as approved by the Institutional Review Board (Hannover Medical School). The isolated cells had been characterized as MSCs by surface marker analysis and functional properties (Dominici et al., 2006). Briefly, cells were characterized by flow cytometry for specific immunotypic MSC markers and were positive for

CD44, CD73, CD90, and CD105, and negative for endothelial (CD31) and hematopoietic (CD34 and CD45) markers. Isolated hAD-MSCs were able to differentiate under controlled conditions toward adipocytes, chondrocytes, and osteocytes (confirmed by Oil Red O, Alcian Blue, and Alizarin Red staining, respectively). AD-MSCs were expanded in  $\alpha$ -minimum essential medium (MEM; Thermo Fisher Scientific, Waltham, MA) containing 1 g/L glucose, 2 mM L-glutamine, 10% human serum, and 50  $\mu$ g/ml gentamicin (Merck KGaA), harvested by Accutase treatment (Merck KGaA) and cryopreserved at Passage 2 until the start of the experiment.

### 2.2 | Plasmid construction and lentivirus production

For lentiviral production, a second-generation lentivirus system was used. We used lentiviral transfer vector pL-CMV-purom backbone replacing the CMV promoter and the CMV enhancer in it with the amplified HRE-dUnaG sequence described previously (Erapanedi et al., 2016). Polymerase chain reaction amplification of HRE-dUnaG was done using specific flanking primers containing restriction sites ClaI and BamHI. HRE-dUnaG sequence consisted of minimal human CMV promoter, which was preceded by five HRE sequence motifs, which drive UnaG expression. The C-terminus of UnaG was in frame with PEST motif-signal for rapid protein degradation.

Lentiviruses were produced in HEK-923T cells. Briefly, HEK-923T cells were seeded into TC-Scale 35 Petri dishes (Sarstedt, Germany) at a density of  $70 \times 10^4$  cells/dish in 3 ml Dulbecco's modified Eagle's medium (DMEM; Merck) supplemented with 3% fetal calf serum (FCS; Merck) without antibiotics. Cells were incubated for 24 hr in a humidified environment at 37°C/5% CO<sub>2</sub>. For transfection of HEK-293T, 0.83  $\mu$ g pMD.G, 3.36  $\mu$ g pL-HRE-dUnaG, 2.8  $\mu$ g plasmid p 8.91, and 20  $\mu$ g polyethyleneimine (1 mg/ml; linear, MW 25 000; PEI 25K; Polysciences Europe GmbH, Hirschberg an der Bergstrasse, Germany) were used. All components were mixed in 500  $\mu$ l of OptiMEM (Thermo Fisher Scientific, Germany), incubated for 5 min at room temperature (RT), and added dropwise to each Petri dish. After 3 hr of incubation, the cell culture medium was exchanged with 3 ml DMEM supplemented with 10% FCS and supernatants were collected after 24 and 48 hr and filtered with 0.45- $\mu$ m syringe filters (Sartorius Stedim, Germany).

### 2.3 | hAD-MSC transduction

hAD-MSCs were revitalized 1 day before transduction in 25-cm<sup>2</sup> cell culture flasks (Sarstedt) at a density of  $20 \times 10^4$  cells/flask. For hAD-MSC transduction, 1 ml of filtered virus-containing supernatant was added directly into the T25 flasks with MSCs in cell culture medium. For higher transduction efficiency, 8  $\mu$ l of 8  $\mu$ g/ml polybrene solution (Sequa-brene; Merck KGaA) was added simultaneously with the virus particles. After 72 hr of cultivation, the cell culture supernatant was discarded, cells were subcultivated and expanded for the next 2 weeks, and cryopreserved at Passage 7.

## 2.4 | Long-term proliferation and differentiation

Native/untreated and transduced hAD-MSCs were plated at a density of 3,000 cells/cm<sup>2</sup> in 25-cm<sup>2</sup> cell culture flasks containing 4 ml  $\alpha$ -MEM medium supplemented with 10% human serum and 50  $\mu$ g/ml gentamicin. Cells were subcultivated two times per week with a seeding density of 3,000 cells/cm<sup>2</sup> over 15 passages. Cell number and viability were evaluated by Trypan Blue exclusion and cumulative cell numbers were calculated. Proliferation and differentiation were evaluated in three independent experiments. For trilineage differentiation, cells were seeded into six-well plates (Sarstedt) at a density of 6,000 cells/cm<sup>2</sup> and cultivated for the next 72 hr until full confluence. After reaching confluence, proliferation medium was removed and osteogenic (5 mM  $\beta$ -glycerophosphate, 0.1  $\mu$ M dexamethasone, 0.2 mM L-ascorbate-2-phosphate, 0.5% gentamicin, and 2.5% hPL in  $\alpha$ -MEM), chondrogenic (StemPro Chondrogenic differentiation kit supplemented with 0.5% gentamicin and 2.5% hPL; Gibco, Germany), and adipogenic (StemMACS™ AdipoDiff medium; Miltenyi Biotech GmbH, Germany) media were added. Cells cultivated in proliferation medium served as control. After 21 days of differentiation in a humidified atmosphere containing 5% CO<sub>2</sub> and 21% O<sub>2</sub> at 37°C (media were exchanged every 3–4 days), cells were washed in phosphate-buffered saline (PBS) and fixed for 15 min at RT with 4% paraformaldehyde for staining. For evaluation of osteogenic differentiation, Alizarin Red staining was used. The fixed cell layers were incubated in Alizarin Red solution (1% Alizarin Red S; Merck) in deionized H<sub>2</sub>O for 15 min at RT. After several washing steps with deionized H<sub>2</sub>O, the red chelates were detected with a microscope. Chondrogenic differentiation was evaluated by Alcian Blue staining (accumulation of proteoglycans in the extracellular matrix). Here, fixed cells were washed twice with PBS, incubated for 3 min in 3% acetic acid at RT, followed by 30 min incubation in Alcian Blue solution (1% Alcian Blue 8GX; Merck) in 3% acetic acid at RT. Cell layers were then washed several times with 3% acetic acid and examined under a microscope. For evaluation of adipogenic differentiation, Oil Red O staining was used.

## 2.5 | Cultivation under oxygen tensions of 2.5%, 5%, and 7.5% O<sub>2</sub>

For experiments under reduced oxygen tensions, cells were plated in six-well-plates (Sarstedt) and cultivated in O<sub>2</sub> controllable incubator Heracell 240i (Thermo Fisher Scientific, Germany). O<sub>2</sub> displacement was attained by N<sub>2</sub> influx; CO<sub>2</sub> was maintained at 5% and temperature at 37°C.

## 2.6 | Flow cytometry and microscopic analysis

In this study, the BD FACSAria™ Fusion (Becton Dickinson, Franklin Lakes, NJ) was used for flow cytometry analysis. Cells were detached and pelleted as described above, and resuspended in PBS for analysis.

The target population was gated and the UnaG protein was excited at 488 nm. The resulting green fluorescence was detected via the FL 1 detector (533/30 nm).

Olympus IX50 Inverted Fluorescence Phase Contrast Microscope (Olympus, Germany) was used for microscopic analysis of the plated cells. To detect UnaG fluorescence, a filter cube with excitation BP 470-490 and emission LP > 515 was used.

## 2.7 | Cultivation of transduced hAD-MSCs with DMSO, insulin, and at varying pH

To evaluate the possible influence of oxygen-independent factors, which were previously shown to be able to regulate HIF-1 stabilization, reporter MSCs were cultivated in the presence of dimethyl sulfoxide (DMSO; apoptosis trigger), insulin, and under varying pH values. Cells were seeded in six-well plates (Sarstedt) under similar conditions as described above. At 80% confluence, the media were changed and media supplemented with varying DMSO (Sigma Aldrich, Germany) or insulin concentrations (Merck) were added. For pH experiments, MES-buffer (Carl Roth, Germany) or lactic acid (Sigma Aldrich) was added to the cultivation media and the resulting pH was determined. After 24 hr of incubation in different media, the cells were detached from the plates, washed with PBS, and their fluorescence was determined by flow cytometry.

## 2.8 | Long-term cultivation under oxygen tension of 2.5%

To evaluate the cell response in longer cultivation under lower (2.5%) oxygen concentrations, cells were seeded in six-well-plates at a density of  $6 \times 10^4$  cells/well (Sarstedt) and cultivated for 72 hr in O<sub>2</sub> controllable incubator Heracell 240i. O<sub>2</sub> displacement was attained by N<sub>2</sub> influx, CO<sub>2</sub> was maintained at 5%, and temperature at 37°C. Cells were then analyzed with the help of flow cytometry at the cultivation time points of 24, 32, 48, 56, and 72 hr.

## 2.9 | Cell encapsulation in hydrogels

Encapsulation and cultivation of cells in hydrogels was performed as previously described (Pepelanova et al., 2018). Briefly, cells were detached from the T-flask, counted in a Neubauer Zählkammer, and pelleted. Reporter cells were resuspended in warm hydrogel and 0.1% (w/v) photoinitiator (Irgacure 2959; Sigma Aldrich) was added. Fifty microliter gel was polymerized in sterile silicon forms (5 mm diameter) in Petri dishes and polymerized at 1.2 J/cm<sup>2</sup> (gelatin-methacryloyl [GelMA] hydrogels) or 1.4 J/cm<sup>2</sup> (PEG-fibrinogen [PF] hydrogel) using a UV irradiation system (Bio-Link®; Vilber Lourmat). The polymerization under the above-described conditions resulted in stiffness of 440 Pa for the GelMA hydrogel and 255 Pa for the PF hydrogel, as determined by oscillatory rheology

(Pepelanova et al., 2018). The hydrogels were transferred to a 24-well plate (Sarstedt) with a single hydrogel construct per well and 500  $\mu$ l of media was added.

## 2.10 | Fluorescence evaluation of reporter hAD-MSCs in 3D

The sensor output was investigated via Z-stack microscopy of the encapsulated hydrogels. The media were removed and the hydrogels were centered in the well. Z-stack pictures over a distance of 30  $\mu$ m were taken by Cytation™ 5 Imaging Multi-Mode Reader (BioTek Instruments) for 390  $\mu$ m from the ground. The following exposure settings were selected: bright field; light emitting diode (LED) intensity: 4; exposure time: 100; gain: 1.1; GFP channel: LED-intensity: 10; exposure time: 235; gain: 15. The resulting images were compressed by the integrated software (Gen5 8.0) with a focus stacking within 3 px.

## 3 | RESULTS

### 3.1 | Lentiviral transduction

To create the hypoxia-reporter cells, the sensor element HRE-dUnaG was stably integrated in the genome of hAD-MSCs via lentiviral transduction. Modified hAD-MSCs were kept in quarantine up to Passage 7 for 2 weeks after transduction, due to German safety regulations designed to ensure the absence of the virus particles in

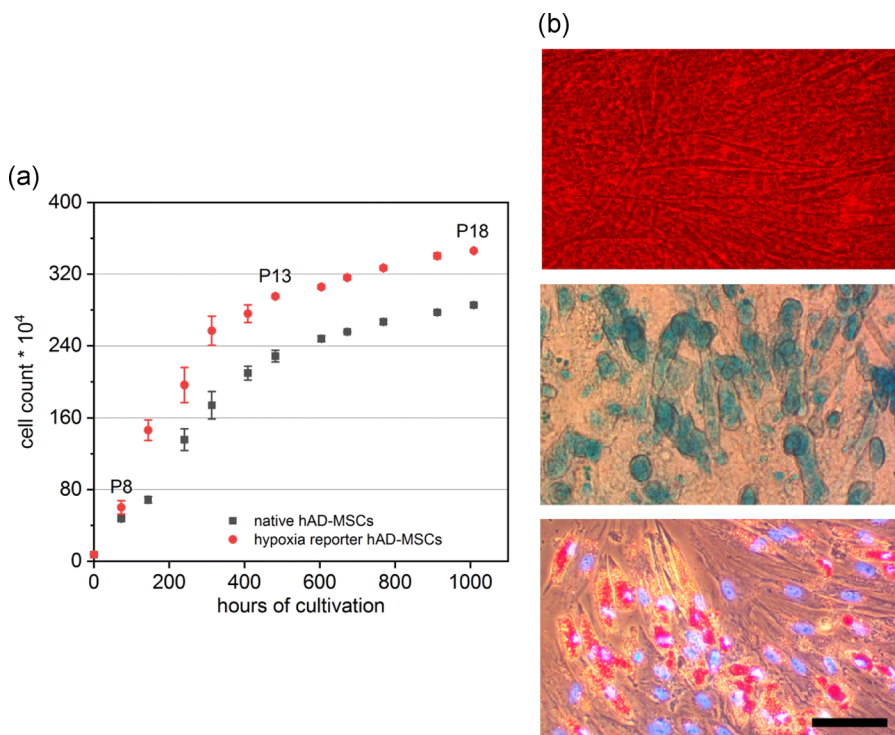
the cell population. Afterwards, the efficiency of transduction was monitored by flow cytometry. First, the total sensor-modified cell population was analyzed by flow cytometry. Then, the cells were cultivated in hypoxia (2.5% O<sub>2</sub>) for 24 hr. After repeated flow cytometry analysis, it was possible to identify 98% of all cells by their fluorescence signal as modified (Figure S1A). The activation of the sensor protein through oxygen deprivation led to an increase in mean fluorescence by over 600 folds. Microscopic analysis, however, showed a certain variance in fluorescence within the hAD-MSC population, likely due to various gene copy numbers integrated per cell (Figure S1B).

### 3.2 | hAD-MSC characterization after modification: Long-term proliferation and differentiation

After reporter cell creation, it was necessary to verify that manipulated MSCs still retain their essential properties despite lentiviral transduction and UnaG expression. Therefore, the cell growth of the reporter cells was compared to the growth of unmodified cells. Long-term proliferation studies demonstrated a slightly higher proliferation rate of manipulated cells in comparison to native hAD-MSCs. Both cell types, however, slowly decreased their proliferation with the increase in the passage numbers as expected. In total, the cells could be subcultivated until Passage 18 (Figure 1a), where they stopped to proliferate.

One of the key characteristics of MSCs is their ability to differentiate into three cell types—osteocytes, chondrocytes, and adipocytes (Dominici et al., 2006). The hypoxia-reporter hAD-MSCs

**FIGURE 1** Hypoxia-reporter human adipose tissue-derived mesenchymal stem cell (hAD-MSC) characterization after lentiviral modification. (a) Proliferation study of hypoxia-reporter hAD-MSCs compared to native hAD-MSCs under ambient oxygen supply. (b) Differentiation of modified hAD-MSCs to osteocytes (top) stained by Alizarin Red, chondrocytes (middle) stained with Alcian Blue, and adipocytes (bottom) stained with Oil Red O and 4',6-diamidino-2-phenylindole. Scale bar: 100  $\mu$ m [Color figure can be viewed at [wileyonlinelibrary.com](http://wileyonlinelibrary.com)]



retained their trilineage differentiation potential, as demonstrated after induction with the corresponding media (Figure 1b). Chondrogenic differentiation was documented by the detection of proteoglycan accumulation with Alcian Blue staining. Positive staining of lipid droplets with Oil Red O demonstrated successful adipogenic differentiation and osteogenic differentiation was confirmed through calcium accumulation visualized with Alizarin Red staining.

### 3.3 | Hypoxia sensor characterization

The reporter cells were cultivated under hypoxia (2.5% O<sub>2</sub>) and fluorescence increase was monitored by both microscopy and flow cytometry. A marked increase in fluorescence signal was detected by flow cytometry after 4 hr of cultivation under 2.5% O<sub>2</sub> supply in the incubator. Also, the analysis showed a linear increase in mean fluorescence over 10 hr of cultivation (Figure 2a). Under the microscope, green fluorescence was detected after 6 hr of cultivation under a 2.5% O<sub>2</sub> supply (Figure 2b).

Earlier, it has been reported that oxygen-independent factors may also induce HIF transactivation (Gaber et al., 2005). These factors include hormones, inflammatory factors, and acidosis. To evaluate the expression of UnaG in modified MSCs under the influence of selected oxygen-independent factors, the reporter hAD-MSCs were incubated for 24 hr in various DMSO (apoptosis trigger) and insulin concentrations. No relevant sensor activation could be observed under the studied conditions (Figure S2). Moreover, exposure to low pH was also tested for sensor activation by two different methods: by cultivating the cells in biological buffer (2-(N-morpholino)ethanesulfonic acid; pH 6.16–7.63) or in high

lactate concentrations. Both methods did not cause an onset of the sensor signal as well (Figure S2C,D).

Reporter cells were then cultured under different oxygen tensions to evaluate the oxygen levels at which UnaG expression and, thus, sensor onset occurs. Modified cells were cultivated for 24 hr under 2.5%, 5%, and 7.5% O<sub>2</sub> and UnaG fluorescence was again analyzed by flow cytometry and microscopy. UnaG fluorescence intensity was found to decrease with an increase of the oxygen tension (Figure 3a,b). After 24 hr at the various oxygen levels, cells were returned to 21% O<sub>2</sub> and the fluorescence response of the sensor was monitored. The decay kinetics of the fluorescence signal are displayed in Figure 4, with higher fluorescence decay rates observed at lower oxygen concentrations. After 48 hr at normoxia, UnaG was completely degraded and no fluorescence could be detected any further. In contrast, if cells were cultivated under reduced oxygen tension (2.5%) over prolonged periods of time (72 hr), the resulting fluorescence signal remained nearly the same as the 24-hr control (Figure S4).

### 3.4 | Hypoxia-reporter cell response in 3D cell culture

To investigate the response of the reporter cells in a 3D culture environment, we embedded the modified hAD-MSCs in photocrosslinkable hydrogels. The influence of encapsulating varying cell concentrations was investigated in two different materials—GelMA (Pepelanova et al., 2018; Shirahama, Lee, Tan, & Cho, 2016) and PF (Almany & Seliktar, 2005). Seeded hydrogel constructs were cultivated under ambient oxygen levels (21% O<sub>2</sub>) for 6 days and visualized with a multimode reader. Z-stack pictures were taken from the bottom of the

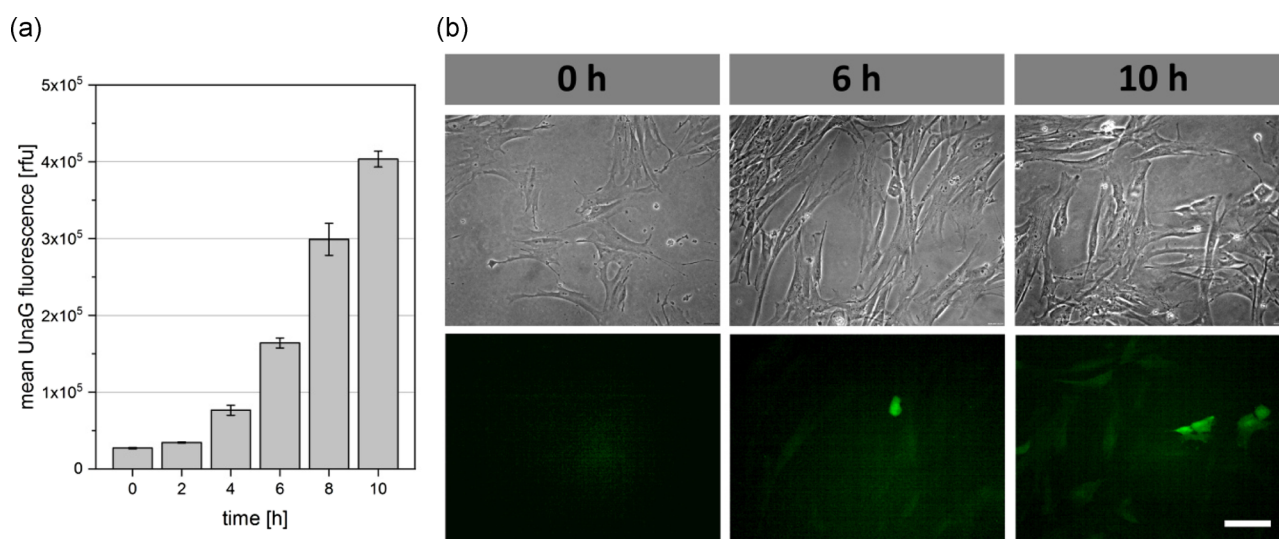


**FIGURE 2** Sensor output of hypoxia-reporter cells after activation under 2.5% O<sub>2</sub>. (a) Flow cytometry analysis of sensor cells cultivated under 2.5% O<sub>2</sub>. Cells were detached every 2 hr for 10 hr and the resulting sensor output was detected immediately. The results show a constant increase of mean UnaG fluorescence. (b) Corresponding microscopic analysis of hypoxia-reporter cells at 0, 6, and 10 hr of cultivation under 2.5% oxygen supply. Scale bar: 100 μm [Color figure can be viewed at [wileyonlinelibrary.com](http://wileyonlinelibrary.com)]

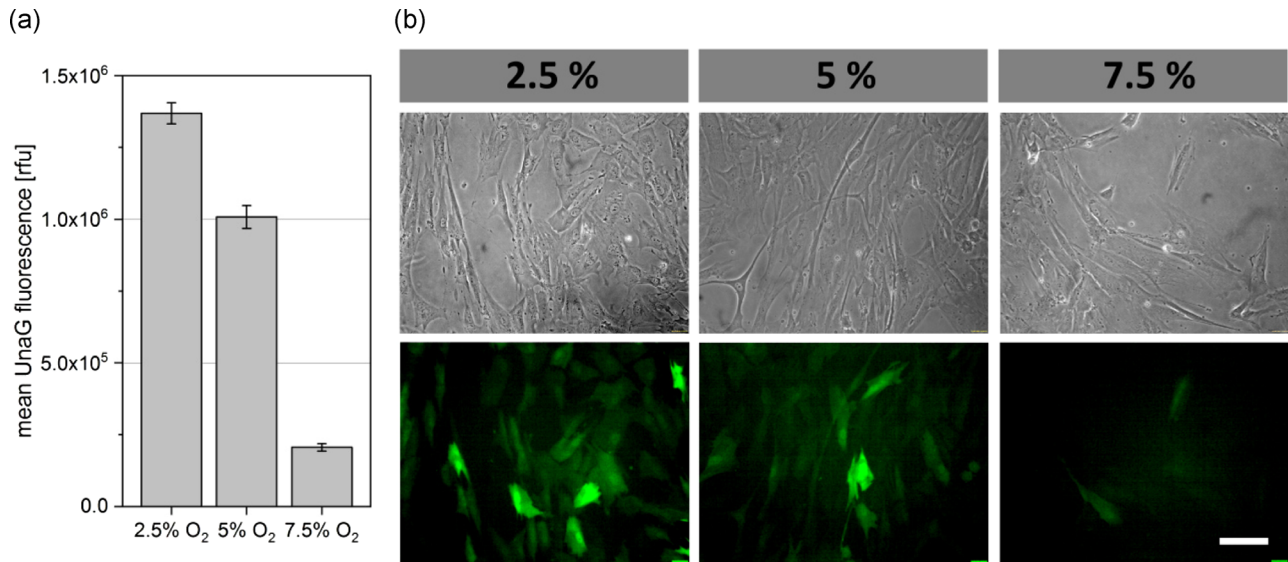


**FIGURE 3** Hypoxia-reporter hAD-MSC activation under various oxygen levels (2.5%, 5%, and 7.5% O<sub>2</sub>). (a) Hypoxia-reporter cells were cultivated under 2.5%, 5%, and 7.5% O<sub>2</sub> for 24 hr and immediately detached from the plate for flow cytometry analysis to detect the mean UnaG fluorescence. (b) Corresponding microscopic analysis of hypoxia-reporter cells after 24 hr of cultivation in various oxygen levels (2.5%, 5%, and 7.5% O<sub>2</sub>) shows a decrease of signal output with increasing oxygen levels. Scale bar: 100  $\mu$ m. hAD-MSC, human adipose tissue-derived mesenchymal stem cell [Color figure can be viewed at [wileyonlinelibrary.com](http://wileyonlinelibrary.com)]

hydrogel construct and reduced to a single image to evaluate the resulting fluorescence of the hypoxia-reporter hAD-MSCs.

In the GelMA hydrogel constructs, individual fluorescent cells could be observed at all cell concentrations, with a significant increase of fluorescence of the cell population at the 8-M/ml level (Figure 5a). The PF hydrogel showed similar tendencies (Figure 5b). Both hydrogel types experienced cell growth-mediated shrinkage during cultivation, which is caused by the high traction forces exerted

by the cells on the matrix (Figure S3). For purposes of better visualization, the complete hydrogel construct was assessed in Figure 5c. The fluorescent frame around each hydrogel was not caused by UnaG expression but occurs due to light refraction during microscopic analysis. A strong hypoxia-reporter signal was mostly detected in the center of the hydrogel constructs, as apparently the highest hypoxic levels occur in the region of strongest oxygen diffusion limitation.

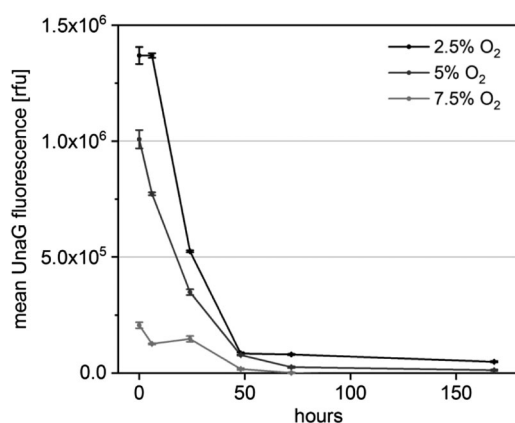


**FIGURE 4** Hypoxia-reporter hAD-MSCs were cultivated under various oxygen levels (2.5%, 5%, and 7.5% O<sub>2</sub>) for 24 hr and reoxygenated to 21% O<sub>2</sub> to investigate the decay kinetics of the sensor output (mean UnaG fluorescence). For flow cytometry, cells were detached and analyzed right after reoxygenation ( $t = 0$  hr) and after 6 hr, 24 hr, 48 hr, 72 hr, and 7 days under ambient oxygen supply. hAD-MSC, human adipose tissue-derived mesenchymal stem cell

## 4 | DISCUSSION

The cultivation of cells in 3D has been repeatedly shown to be a more accurate approximation of the natural cellular environment (Edmondson, Broglie, Adcock, & Yang, 2014; Zoetemelk, Rausch, Colin, Dormond, & Nowak-Sliwinska, 2019). The development of tools for the online monitoring of in situ cell state plays an important role in the understanding of cell biology (Hong, Yang, & Cai, 2011). However, the analytic options for cell behavior evaluation in 3D are often limited to microscopic analysis. In addition, commonly used readouts are not dynamic, but constitute endpoint measurements after cell fixation and staining. Significant variation in experimental outcomes results due to the large number of nonstandardized protocols related to cell encapsulation, cell-seeding numbers, hydrogel types, and cultivation duration. All these drawbacks in current 3D cell culture protocols and analysis can be addressed by the use of integrated intracellular sensors. These are directly sensitive to environmental changes and can serve as a reliable tool for the evaluation of cell state in in vitro 3D cell systems, as well as for in vivo experiments (Erapaneedi et al., 2016).

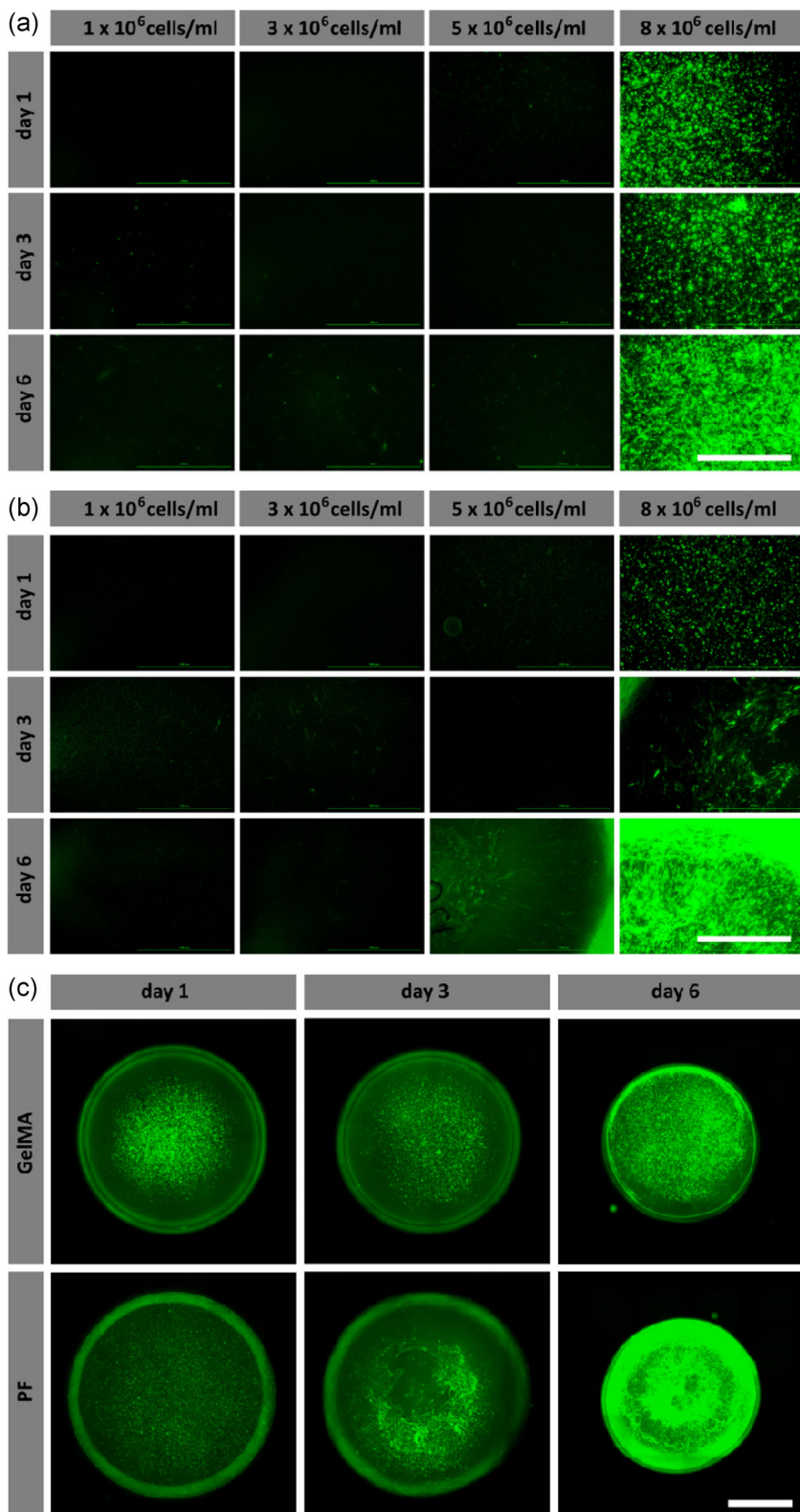


**FIGURE 5** Application of hypoxia-reporter cells in bulk hydrogels. Various concentrations of hypoxia-reporter cells ( $1$ ,  $3$ ,  $5$ , and  $8$  M cells/ml) were encapsulated in (a) gelatin-methacryloyl (GelMA) or (b) PEG-fibrinogen (PF) hydrogel and cultivated under ambient oxygen levels in the incubator over 6 days. As a result of oxygen diffusion through the hydrogels and metabolic oxygen consumption, the hypoxia-reporter cells were activated and the resulting signal output was detected by Z-stack scanning through the hydrogel construct. Scale bar:  $500 \mu\text{m}$ . (c) Full hydrogel evaluation of hypoxia-reporter cell signal output for GelMA and PF-hydrogels with 8 M cells/ml over 6 days of cultivation, showing the increase in signal intensity and the decrease in hydrogel diameter caused by high traction forces through the cells. Scale bar:  $2,000 \mu\text{m}$  [Color figure can be viewed at [wileyonlinelibrary.com](http://wileyonlinelibrary.com)]

Earlier, Erapanedi et al. (2016) demonstrated that HRE-dUnaG sensors transiently integrated in CHO cells were sensitive to changing oxygen concentrations and can be utilized to visualize hypoxic areas when reporter cells were implanted in mice. In our study, we put the focus on hAD-MSCs as the most frequently used cell type in

tissue engineering and bioregenerative medicine. It is important to note, that not only oxygen consumption rates vary between different cell types, but also that the metabolic state of the cells themselves affects in situ oxygen concentrations. For example, MSCs in quiescence do not metabolize as much oxygen as cells in the exponential



growth phase (Wagner, Venkataraman, & Buettner, 2011). Earlier, it was demonstrated that MSCs cultivated under 21% O<sub>2</sub> have an oxygen consumption rate of  $33.1 \pm 2.5 \text{ pmol O}_2 \text{ s}^{-1} \cdot 10^{-6} \text{ cells}$  (Hughey et al., 2012). Thus, it is important to evaluate the hypoxic response of different cell types and to place this finding in the metabolic context of each cell.

In this study, we integrated a genetically encoded hypoxia sensor in hAD-MSCs, which is activated by HIF-1 $\alpha$ -stabilization (Majmundar, Wong, & Simon, 2010). Modification of hAD-MSCs with the hypoxia sensor did not affect their stem cell-related properties—cells were able to differentiate into chondrocytes, adipocytes, and osteocytes. Long-term proliferation of the cells with integrated sensor, however, was slightly higher in comparison to nonmodified cells. Maintenance of native MSC properties after lentiviral transduction is essential, since it was demonstrated that such manipulation can lead to MSC alterations (Von Der Haar et al., 2019). Our experiments could show that the stemness of cells is retained after manipulation with the lentiviral vector.

The hypoxic sensor was successfully activated by cultivating the reporter cells under oxygen deprivation. A return to normoxia (21% O<sub>2</sub>) led to rapid decay of fluorescence related to the degradation of the reporter protein UnaG. Fast reporter protein degradation is crucial for reliable real-time cell monitoring, as it is able to provide readout of adequate temporal resolution. UnaG protein fluorescence, as well as degradation rate, was inversely related to the oxygen tension in the incubator: the lower the oxygen level to which the reporter cells were subjected, the higher UnaG fluorescence was measured with flow cytometry. Flow cytometry analysis was shown to be more sensitive for detecting sensor onset than microscopy, which has been used earlier for a similar sensor in CHO cells (Erapaneedi et al., 2016). We also tested the influence of insulin, pH, and DMSO (as an activator of apoptosis) on the sensor onset, as these factors are closely related to HIF stabilization (Gaber et al., 2005). Earlier, HIF activation by pH-dependent nuclear sequestration of VHL was reported (Mekhail, Gunaratnam, Bonicalzi, & Lee, 2004). Also, insulin was shown to be able to induce the transcription of HIF target genes (Feldser et al., 1999; Zelzer et al., 1998). No activation patterns were observed in the modified hAD-MSCs by these external stimuli. This confirms that the activation of the genetic reporter construct strongly depends on hypoxic culture conditions alone.

The reporter cells were encapsulated in two different hydrogel types to create a 3D cellular environment. There is great availability of hydrogels with diverse biomechanical properties which may influence the state of the embedded cells. Stiffness, pore size, and crosslinking method are significant factors when choosing the most appropriate hydrogel for a specific experiment. GelMA hydrogels are a popular 3D cultivation platform since they show great tunability, allow for cell adhesion via the presence of RGD motifs, and can be modulated by the cells over time (Lin, Su, Lee, & Lin, 2018; Visser et al., 2015; Xiao et al., 2019). In our experiments, we chose a hydrogel concentration of 5% GelMA (w/v), as it has been shown before that MSCs maintain high viability and display spreading at this concentration (Nichol et al., 2010). PF hydrogel represents another

photo-crosslinkable hydrogel system, which also has a great track record for MSC cultivation (Yosef et al., 2019). PF hydrogel also possesses many adhesion sites for cell attachment and migration, and its mechanical properties can be tuned by adapting the level of cross-linker (Cohen et al., 2018; Rufaihah et al., 2018). Various cell numbers of hypoxia-reporter hAD-MSCs were seeded in the two different hydrogel systems and the sensor onset was investigated. The most significant sensor onset was detected by a cell concentration of 8 M cells/ml in each case. Other groups have also researched oxygen availability in relation to the seeded cell number. For instance, Demol, Lambrechts, Geris, Schrooten, and Van Oosterwyck (2011) created mathematical models of oxygen availability in cell-loaded fibrin hydrogels and verified the model applicability in vitro, showing that even constructs within 1 M cells/ml hydrogel experience a significant drop of oxygen with increasing hydrogel depth and with elongated cultivation time. These findings were supported by Sachlos, Czernuszka, Gogolewski, and Dalby (2003) who stated that oxygen supply in 3D tissues is crucial for any kind of tissue engineering application and that the limited penetration depth of oxygen and nutrients inhibits the growth of cells in deep tissue layers. In our study, we could demonstrate that the onset of hypoxia (HIF-1 $\alpha$  stabilization) in the bulk hydrogel constructs of 50  $\mu\text{l}$  appears with significantly higher cell-seeding numbers.

Cells exhibited high traction forces on the hydrogel matrix, which led to construct shrinkage over the cultivation period of 6 days. The shrinking of hydrogels by cells has been demonstrated by other working groups and its extent depends on the mechanical and compositional properties of the materials used (Ahearne, Wilson, Liu, Haj, & Rauz, 2009; Mauck, Wang, Oswald, Ateshian, & Hung, 2003). A change in the hydrogels' shape and diameter led to more compressed constructs after 6 days of cultivation, which influenced the intensity of the resulting fluorescence in the microscopic images.

The precise knowledge of the onset of hypoxia in hydrogel constructs by the seeding of specific cell numbers is a vital piece of biological information. It helps avoid hypoxia if undesirable, by going down to seeding lower cell numbers. Moreover, variation of seeded cell number can help create hypoxic microenvironments in 3D cultures without changing oxygen levels in the overhead of the cell incubator. In our experiments, the seeding of 8 M cells/ml reduced oxygen availability by oxygen consumption, thus inducing hypoxia without the help of external oxygen control. While it is well known that gradients of all kinds exist in a diffusion-limited environments loaded with cells (Murphy & O'Brien, 2010), for the first time it was possible to noninvasively observe oxygen deprivation as a result of seeded cell numbers.

We suggest that hypoxia-reporter cells can be used to estimate the in situ oxygen availability in cell culture applications. These modified reporter cells would be superior to direct oxygen measurements in hydrogels, since stabilization of HIF-1 $\alpha$  can be influenced by a variety of complex factors, beyond oxygen tension (Semenza, 2017). Although we could demonstrate that the onset of fluorescence of the sensor is not influenced by pH, lactate concentrations, insulin, and apoptosis, additional factors such as

cell-matrix interactions, redox state of the cells, as well as the presence of small molecules can play a role in the stabilization of HIF-1 $\alpha$  together with lower oxygen levels (Gaber et al., 2005). Considering that HIF-1 $\alpha$  stabilization regulates the expression of over 300 genes involved in cell signaling, metabolic activity, and cytokine expression, the knowledge of the cell state in 3D in vitro constructs provides essential information for data analysis (Liu, Shen, Zhao, & Chen, 2012). In future studies, the hypoxia-reporter hAD-MSCs must be tested under different cultivation conditions, such as, for example, differentiation. For example, Shum, White, Mills, De Mesy Bentley, and Eliseev (2016) demonstrated that HIF-1 $\alpha$  is downregulated when osteogenesis is induced in MSCs, thus indicating that sensor activation might be different after differentiation. Furthermore, the application of sensor-modified cells in cocultures with different cell types (e.g., human umbilical vein endothelial cells or chondrocytes) could clarify if the onset of hypoxia has an influence on the microvascular networks or cartilage formation (Carrion et al., 2010) in complex 3D models. Another improvement would be the use of fluorescence-activated cell sorting to obtain a more homogenous population of the hypoxia-reporting cells. In a more homogenous sensor cell population, even the fluorescent intensity of a single cell will be able to indicate a specific range of in situ oxygen concentrations. Additionally, microscopic algorithms for fluorescence quantification can be applied on a 3D construct, thus evaluating changes in hypoxia over the entire cell population. Alternatively, the release of encapsulated cells from hydrogels with subsequent flow cytometry evaluation can also allow for precise fluorescence quantification. In the current study, UnaG expression is heterogenic throughout the whole cell population and it remains unclear if this is due to variation in gene copy number integration or due to a variability of the hypoxic response of singular cells in a heterogenic population of MSCs. This question must be explored in future studies. Additionally, the reporter cell response on even lower oxygen concentrations (1% and less) should be evaluated in the future in both 2D and 3D cell cultures. While our research group mostly focuses on hypoxia, the HRE-dUnaG construct might even prove useful in cancer research which investigates pseudohypoxia, a state of malignant cells where HIF is permanently stabilized (Shum et al., 2016).

Finally, it is important to reflect on the fact that cells growing in 3D never really truly experience homogenous growth conditions. Indeed, various gradients, such as oxygen gradients and gradients of released proteins or metabolites will always make a 3D construct inhomogeneous. For reliable evaluation of the 3D constructs, relevant tools for cell-state assessment must be established. Hypoxia-reporting MSCs might be the first step to a better understanding of cell behavior in such systems.

## ACKNOWLEDGMENTS

This study was supported by the German Research Foundation (DFG Project 398007461 488 "3D Dual-Gradient Systems for Functional Cell Screening") and Grant # 075-15-2019-1789 from the Ministry of Science and Higher Education of the Russian Federation. The publication of this article was funded by the Open Access Fund of Leibniz

Universität Hannover. The authors also want to acknowledge support by the SMART BIOTECS initiative, financially supported by the Ministry of Science and Culture (MWK) of Lower Saxony, Germany. Open access funding enabled and organized by Projekt DEAL.

## ORCID

Carola Schmitz  <http://orcid.org/0000-0001-5337-299X>

Dror Seliktar  <https://orcid.org/0000-0001-6964-8567>

Antonina Lavrentieva  <https://orcid.org/0000-0003-0003-5572>

## REFERENCES

- Ahearne, M., Wilson, S., Liu, I. K. K., Haj, A., & Rauz, S. (2009). Influence of cell number and collagen concentration on the mechanical behaviour of collagen hydrogel constructs. *European Cells and Materials*, 18, 21.
- Almany, L., & Seliktar, D. (2005). Biosynthetic hydrogel scaffolds made from fibrinogen and polyethylene glycol for 3D cell cultures. *Biomaterials*, 26(15), 2467–2477. <https://doi.org/10.1016/j.biomaterials.2004.06.047>
- Bahoun, S., Coopman, K., Forsyth, N. R., & Akam, E. C. (2018). The role of dissolved oxygen levels on human mesenchymal stem cell culture success, regulatory compliance, and therapeutic potential. *Stem Cells and Development*, 27(19), 1303–1321. <https://doi.org/10.1089/scd.2017.0291>
- Carrion, B., Huang, C. P., Ghajar, C. M., Kachgal, S., Kniazeva, E., Jeon, N. L., & Putnam, A. J. (2010). Recreating the perivascular niche ex vivo using a microfluidic approach. *Biotechnology and Bioengineering*, 107(6), 1020–1028. <https://doi.org/10.1002/bit.22891>
- Chakraborty, A. A., Laukka, T., Myllykoski, M., Ringel, A. E., Booker, M. A., Tolstorukov, M. Y., ... Kaelin, W. G. (2019). Histone demethylase KDM6A directly senses oxygen to control chromatin and cell fate. *Science*, 363, 1217–1222. <https://doi.org/10.1126/science.aaw1026>
- Cheng, N. C., Chen, S. Y., Li, J. R., & Young, T. H. (2013). Short-term spheroid formation enhances the regenerative capacity of adipose-derived stem cells by promoting stemness, angiogenesis, and chemotaxis. *Stem Cells Translational Medicine*, 2(8), 584–594. <https://doi.org/10.5966/sctm.2013-0007>
- Choi, J. R., Yong, K. W., & Wan Safwani, W. K. Z. (2017). Effect of hypoxia on human adipose-derived mesenchymal stem cells and its potential clinical applications. *Cellular and Molecular Life Sciences*, 74, 2587–2600. <https://doi.org/10.1007/s00018-017-2484-2>
- Cohen, N., Toister, E., Lati, Y., Girshengorn, M., Levin, L., Silberstein, L., ... Epstein, E. (2018). Cell encapsulation utilizing PEG-fibrinogen hydrogel supports viability and enhances productivity under stress conditions. *Cytotechnology*, 70(3), 1075–1083. <https://doi.org/10.1007/s10616-018-0204-x>
- Demol, J., Lambrechts, D., Geris, L., Schrooten, J., & Van Oosterwyck, H. (2011). Towards a quantitative understanding of oxygen tension and cell density evolution in fibrin hydrogels. *Biomaterials*, 32(1), 107–118. <https://doi.org/10.1016/j.biomaterials.2010.08.093>
- Dominici, M., Le Blanc, K., Mueller, I., Slaper-Cortenbach, I., Marini, F. C., Krause, D. S., ... Horwitz, E. M. (2006). Minimal criteria for defining multipotent mesenchymal stromal cells. The International Society for Cellular Therapy position statement. *Cytotherapy*, 8(4), 315–317. <https://doi.org/10.1080/14653240600855905>
- Edmondson, R., Broglie, J. J., Adcock, A. F., & Yang, L. (2014). Three-dimensional cell culture systems and their applications in drug discovery and cell-based biosensors. *Assay and Drug Development Technologies*, 12(4), 207–218. <https://doi.org/10.1089/adt.2014.573>
- Ejtehadifar, M., Shamsasenjan, K., Movassaghpour, A., Akbarzadehlaleh, P., Dehdilani, N., Abbasi, P., ... Saleh, M. (2015). The effect of hypoxia on mesenchymal stem cell biology. *Advanced Pharmaceutical Bulletin*, 5(2), 141–149. <https://doi.org/10.15171/apb.2015.021>
- Erapaneedi, R., Belousov, V. V., Schäfers, M., & Kiefer, F. (2016). A novel family of fluorescent hypoxia sensors reveal strong heterogeneity in

- tumor hypoxia at the cellular level. *The EMBO Journal*, 35(1), 102–113. <https://doi.org/10.15252/embj.201592775>
- Feldser, D., Agani, F., Iyer, N. V., Pak, B., Ferreira, G., & Semenza, G. L. (1999). Reciprocal positive regulation of hypoxia-inducible factor 1 $\alpha$  and insulin-like growth factor 2. *Cancer Research*, 59(16–18).
- Figueiredo, L., Pace, R., D'Arros, C., Réthoré, G., Guicheux, J., Le Visage, C., & Weiss, P. (2018). Assessing glucose and oxygen diffusion in hydrogels for the rational design of 3D stem cell scaffolds in regenerative medicine. *Journal of Tissue Engineering and Regenerative Medicine*, 12(5), 1238–1246. <https://doi.org/10.1002/term.2656>
- Fábián, Z. (2019). The effects of hypoxia on the immune-modulatory properties of bone marrow-derived mesenchymal stromal cells. *Stem Cells International*, 2019, 2509606. <https://doi.org/10.1155/2019/2509606>
- Gaber, T., Dziurla, R., Tripmacher, R., Burmester, G. R., & Buttgerit, F. (2005). Hypoxia inducible factor (HIF) in rheumatology: Low O<sub>2</sub>! See what HIF can do! *Annals of the Rheumatic Diseases*, 64(7), 971–980. <https://doi.org/10.1136/ard.2004.031641>
- Han, Y., Li, X., Zhang, Y., Han, Y., Chang, F., & Ding, J. (2019). Mesenchymal stem cells for regenerative medicine. *Cells*, 8(8), 886. <https://doi.org/10.3390/cells8080886>
- Haque, N., Rahman, M. T., Abu Kasim, N. H., & Alabsi, A. M. (2013). Hypoxic culture conditions as a solution for mesenchymal stem cell based regenerative therapy. *The Scientific World Journal*, 2013, 632972. <https://doi.org/10.1155/2013/632972>
- Hong, H., Yang, Y., & Cai, W. (2011). Imaging gene expression in live cells and tissues. *Cold Spring Harbor Protocols*, 6(4), pdb.top103. <https://doi.org/10.1101/pdb.top103>
- Hu, W., Wang, Z., Xiao, Y., Zhang, S., & Wang, J. (2019). Advances in crosslinking strategies of biomedical hydrogels. *Biomaterials Science*, 7(3), 843–855. <https://doi.org/10.1039/c8bm01246f>
- Hu, X., Yu, S. P., Fraser, J. L., Lu, Z., Ogle, M. E., Wang, J. A., & Wei, L. (2008). Transplantation of hypoxia-preconditioned mesenchymal stem cells improves infarcted heart function via enhanced survival of implanted cells and angiogenesis. *Journal of Thoracic and Cardiovascular Surgery*, 135, 799–808. <https://doi.org/10.1016/j.jtcvs.2007.07.071>
- Hughey, C. C., Alfaro, M. P., Belke, D. D., Rottman, J. N., Young, P. P., Wasserman, D. H., & Shearer, J. (2012). Increased oxygen consumption and OXPHOS potential in superhealer mesenchymal stem cells. *Cell Regeneration*, 1(1), 3. <https://doi.org/10.1186/2045-9769-1-3>
- Ivanovic, Z. (2009). Hypoxia or in situ normoxia: The stem cell paradigm. *Journal of Cellular Physiology*, 219, 271–275. <https://doi.org/10.1002/jcp.21690>
- Jiang, B. H., Rue, E., Wang, G. L., Roe, R., & Semenza, G. L. (1996). Dimerization, DNA binding, and transactivation properties of hypoxia-inducible factor 1. *Journal of Biological Chemistry*, 271(30), 17771–17778. <https://doi.org/10.1074/jbc.271.30.17771>
- Koh, M. Y., & Powis, G. (2012). Passing the baton: The HIF switch. *Trends in Biochemical Sciences*, 37, 364–372. <https://doi.org/10.1016/j.tibs.2012.06.004>
- Kumagai, A., Ando, R., Miyatake, H., Greimel, P., Kobayashi, T., Hirabayashi, Y., ... Miyawaki, A. (2013). A bilirubin-inducible fluorescent protein from eel muscle. *Cell*, 153(7), 1602–1611. <https://doi.org/10.1016/j.cell.2013.05.038>
- Lavrentieva, A., Majore, I., Kasper, C., & Hass, R. (2010). Effects of hypoxic culture conditions on umbilical cord-derived human mesenchymal stem cells. *Cell Communication and Signaling*, 8, 1–9. <https://doi.org/10.1186/1478-811X-8-18>
- Lin, C. H., Su, J. J. M., Lee, S. Y., & Lin, Y. M. (2018). Stiffness modification of photopolymerizable gelatin-methacrylate hydrogels influences endothelial differentiation of human mesenchymal stem cells. *Journal of Tissue Engineering and Regenerative Medicine*, 12(10), 2099–2111. <https://doi.org/10.1002/term.2745>
- Liu, W., Shen, S. M., Zhao, X. Y., & Chen, G. Q., Dr. (2012). Targeted genes and interacting proteins of hypoxia inducible factor-1. *International Journal of Biochemistry and Molecular Biology*, 3(2), 165–178.
- Lukomska, B., Stanaszek, L., Zuba-Surma, E., Legosz, P., Sarzynska, S., & Drela, K. (2019). Challenges and controversies in human mesenchymal stem cell therapy. *Stem Cells International*, 2019, 2019. <https://doi.org/10.1155/2019/9628536>
- Lönne, M., Lavrentieva, A., Walter, J. G., & Kasper, C. (2013). Analysis of oxygen-dependent cytokine expression in human mesenchymal stem cells derived from umbilical cord. *Cell and Tissue Research*, 353(1), 117–122. <https://doi.org/10.1007/s00441-013-1597-7>
- Majmundar, A. J., Wong, W. J., & Simon, M. C. (2010). Hypoxia-inducible factors and the response to hypoxic stress. *Molecular Cell*, 40(2), 294–309. <https://doi.org/10.1016/j.molcel.2010.09.022>
- Malda, J., Visser, J., Melchels, F. P., Jüngst, T., Hennink, W. E., Dhert, W. J. A., ... Huttmacher, D. W. (2013). 25th anniversary article: Engineering hydrogels for biofabrication. *Advanced Materials*, 25(36), 5011–5028. <https://doi.org/10.1002/adma.201302042>
- Mauck, R. L., Wang, C. C. B., Oswald, E. S., Ateshian, G. A., & Hung, C. T. (2003). The role of cell seeding density and nutrient supply for articular cartilage tissue engineering with deformational loading. *Osteoarthritis and Cartilage*, 11(12), 879–890. <https://doi.org/10.1016/j.joca.2003.08.006>
- Maxwell, P. H., Wlesener, M. S., Chang, G. W., Clifford, S. C., Vaux, E. C., Cockman, M. E., ... Ratcliffe, P. J. (1999). The tumour suppressor protein VHL targets hypoxia-inducible factors for oxygen-dependent proteolysis. *Nature*, 399(6733), 271–275. <https://doi.org/10.1038/20459>
- Mekhail, K., Gunaratnam, L., Bonicalzi, M. E., & Lee, S. (2004). HIF activation by pH-dependent nucleolar sequestration of VHL. *Nature Cell Biology*, 6, 642–647. <https://doi.org/10.1038/ncb1144>
- Murphy, C. M., & O'Brien, F. J. (2010). Understanding the effect of mean pore size on cell activity in collagen-glycosaminoglycan scaffolds. *Cell Adhesion & Migration*, 4(3), 377–381. <https://doi.org/10.4161/cam.4.3.11747>
- Nichol, J. W., Koshy, S. T., Bae, H., Hwang, C. M., Yamanlar, S., & Khademhosseini, A. (2010). Cell-laden microengineered gelatin methacrylate hydrogels. *Biomaterials*, 31(21), 5536–5544. <https://doi.org/10.1016/j.biomaterials.2010.03.064>
- Pagé, E. L., Robitaille, G. A., Pouyssegur, J., & Richard, D. E. (2002). Induction of hypoxia-inducible factor-1 $\alpha$  by transcriptional and translational mechanisms. *Journal of Biological Chemistry*, 277(50), 48403–48409. <https://doi.org/10.1074/jbc.M209114200>
- Pattappa, G., Johnstone, B., Zellner, J., Docheva, D., & Angele, P. (2019). The importance of physioxia in mesenchymal stem cell chondrogenesis and the mechanisms controlling its response. *International Journal of Molecular Sciences*, 20(3), 484.
- Pepelanova, I., Kruppa, K., Scheper, T., & Lavrentieva, A. (2018). Gelatin-methacryloyl (GelMA) hydrogels with defined degree of functionalization as a versatile toolkit for 3D cell culture and extrusion bioprinting. *Bioengineering*, 5(3), <https://doi.org/10.3390/bioengineering5030055>
- Pugh, C. W., & Ratcliffe, P. J. (2017). New horizons in hypoxia signaling pathways. *Experimental Cell Research*, 356(2), 116–121. <https://doi.org/10.1016/j.yexcr.2017.03.008>
- Ruedinger, F., Lavrentieva, A., Blume, C., Pepelanova, I., & Scheper, T. (2015). Hydrogels for 3D mammalian cell culture: A starting guide for laboratory practice. *Applied Microbiology and Biotechnology*, 99(2), 623–636. <https://doi.org/10.1007/s00253-014-6253-y>
- Rufaihah, A. J., Cheyyatraivendran, S., Mazlan, M. D. M., Lim, K., Chong, M. S. K., Mattar, C. N. Z., ... Seliktar, D. (2018). The effect of scaffold modulus on the morphology and remodeling of fetal mesenchymal stem cells. *Frontiers in Physiology*, 9(December), 1–20. <https://doi.org/10.3389/fphys.2018.01555>
- Sachlos, E., Czernuszka, J. T., Gogolewski, S., & Dalby, M. (2003). Making tissue engineering scaffolds work. Review on the application of solid

- freeform fabrication technology to the production of tissue engineering scaffolds. *European Cells and Materials*, 5, 29–40. <https://doi.org/10.22203/ecm.v005a03>
- Schödel, J., Oikonomopoulos, S., Ragoussis, J., Pugh, C. W., Ratcliffe, P. J., & Mole, D. R. (2011). High-resolution genome-wide mapping of HIF-binding sites by ChIP-seq. *Blood*, 117(23), e207–e217. <https://doi.org/10.1182/blood-2010-10-314427>
- Semenza, G. L. (2017). A compendium of proteins that interact with HIF-1 $\alpha$ . *Experimental Cell Research*, 356(2), 128–135. <https://doi.org/10.1016/j.physbeh.2017.03.040>
- Shirahama, H., Lee, B. H., Tan, L. P., & Cho, N. J. (2016). Precise tuning of facile one-pot gelatin methacryloyl (GelMA) synthesis. *Scientific Reports*, 6(July), 1–11. <https://doi.org/10.1038/srep31036>
- Shum, L. C., White, N. S., Mills, B. N., De Mesy Bentley, K. L., & Eliseev, R. A. (2016). Energy metabolism in mesenchymal stem cells during osteogenic differentiation. *Stem Cells and Development*, 25(2), 114–122. <https://doi.org/10.1089/scd.2015.0193>
- Visser, J., Gawlitta, D., Benders, K. E. M., Toma, S. M. H., Poursan, B., van Weeren, P. R., ... Malda, J. (2015). Endochondral bone formation in gelatin methacrylamide hydrogel with embedded cartilage-derived matrix particles. *Biomaterials*, 37, 174–182. <https://doi.org/10.1016/j.biomaterials.2014.10.020>
- Von Der Haar, K., Jonczyk, R., Lavrentieva, A., Weyand, B., Vogt, P., Jochums, A., ... Blume, C. A. (2019). Electroporation: A sustainable and cell biology preserving cell labeling method for adipogenous mesenchymal stem cells. *BioResearch Open Access*, 8(1), 32–44. <https://doi.org/10.1089/biores.2019.0001>
- Wagner, B. A., Venkataraman, S., & Buettner, G. R. (2011). The rate of oxygen utilization by cells. *Free Radical Biology and Medicine*, 51, 700–712. <https://doi.org/10.1016/j.freeradbiomed.2011.05.024>
- Wenger, R., Kurtcuoglu, V., Scholz, C., Marti, H., & Hoogewijs, D. (2015). Frequently asked questions in hypoxia research. *Hypoxia*, 3, 35–43. <https://doi.org/10.2147/hp.s92198>
- Xiao, S., Zhao, T., Wang, J., Wang, C., Du, J., Ying, L., ... Xu, K. (2019). Gelatin methacrylate (GelMA)-based hydrogels for cell transplantation: An effective strategy for tissue engineering. *Stem Cell Reviews and Reports*, 15(5), 664–679. <https://doi.org/10.1007/s12015-019-09893-4>
- Yamamoto, Y., Fujita, M., Tanaka, Y., Kojima, I., Kanatani, Y., Ishihara, M., & Tachibana, S. (2013). Low oxygen tension enhances proliferation and maintains stemness of adipose tissue-derived stromal cells. *BioResearch Open Access*, 2(3), 199–205. <https://doi.org/10.1089/biores.2013.0004>
- Yosef, A., Kossover, O., Mironi-Harpaz, I., Mauretti, A., Melino, S., Mizrahi, J., & Seliktar, D. (2019). Fibrinogen-based hydrogel modulus and ligand density effects on cell morphogenesis in two-dimensional and three-dimensional cell cultures. *Advanced Healthcare Materials*, 8(13), 1–13. <https://doi.org/10.1002/adhm.201801436>
- Zelzer, E., Levy, Y., Kahana, C., Shilo, B. Z., Rubinstein, M., & Cohen, B. (1998). Insulin induces transcription of target genes through the hypoxia-inducible factor HIF-1 $\alpha$ /ARNT. *EMBO Journal*, 17, 5085–5094. <https://doi.org/10.1093/emboj/17.17.5085>
- Zhu, Y., Liu, T., Song, K., Fan, X., Ma, X., & Cui, Z. (2008). Adipose-derived stem cell: A better stem cell than BMSC. *Cell Biochemistry and Function*, 26, 664–675. <https://doi.org/10.1002/cbf.1488>
- Zoetemelk, M., Rausch, M., Colin, D. J., Dormond, O., & Nowak-Sliwinska, P. (2019). Short-term 3D culture systems of various complexity for treatment optimization of colorectal carcinoma. *Scientific Reports*, 9(1), 1–14. <https://doi.org/10.1038/s41598-019-42836-0>

## SUPPORTING INFORMATION

Additional supporting information may be found online in the Supporting Information section.

**How to cite this article:** Schmitz C, Pepelanova I, Seliktar D, et al. Live reporting for hypoxia: Hypoxia sensor-modified mesenchymal stem cells as in vitro reporters. *Biotechnology and Bioengineering*. 2020;117:3265–3276. <https://doi.org/10.1002/bit.27503>